

REVIEW

Open Access



Two-dimensional metal-organic frameworks: from synthesis to bioapplications

Weiqi Wang¹ , Yuting Yu¹, Yilan Jin¹, Xiao Liu¹, Min Shang¹, Xiaohua Zheng^{1*}, Tingting Liu^{2*} and Zhigang Xie^{3*}

Abstract

As a typical class of crystalline porous materials, metal–organic framework possesses unique features including versatile functionality, structural and compositional tunability. After being reduced to two-dimension, ultrathin metal-organic framework layers possess more external excellent properties favoring various technological applications. In this review article, the unique structural properties of the ultrathin metal-organic framework nanosheets benefiting from the planar topography were highlighted, involving light transmittance, and electrical conductivity. Moreover, the design strategy and versatile fabrication methodology were summarized covering discussions on their applicability and accessibility, especially for porphyritic metal-organic framework nanosheet. The current achievements in the bio-applications of two-dimensional metal-organic frameworks were presented comprising biocatalysis, biosensor, and theranostic, with an emphasis on reactive oxygen species-based nanomedicine for oncology treatment. Furthermore, current challenges confronting the utilization of two-dimensional metal-organic frameworks and future opportunities in emerging research frontiers were presented.

Keywords: Metal-organic framework, Two-dimensional materials, Diagnostic, Biosensing, Cancer treatment

*Correspondence: xiaohuaz@ntu.edu.cn; liutingting810418@foxmail.com;
xiez@ciac.ac.cn

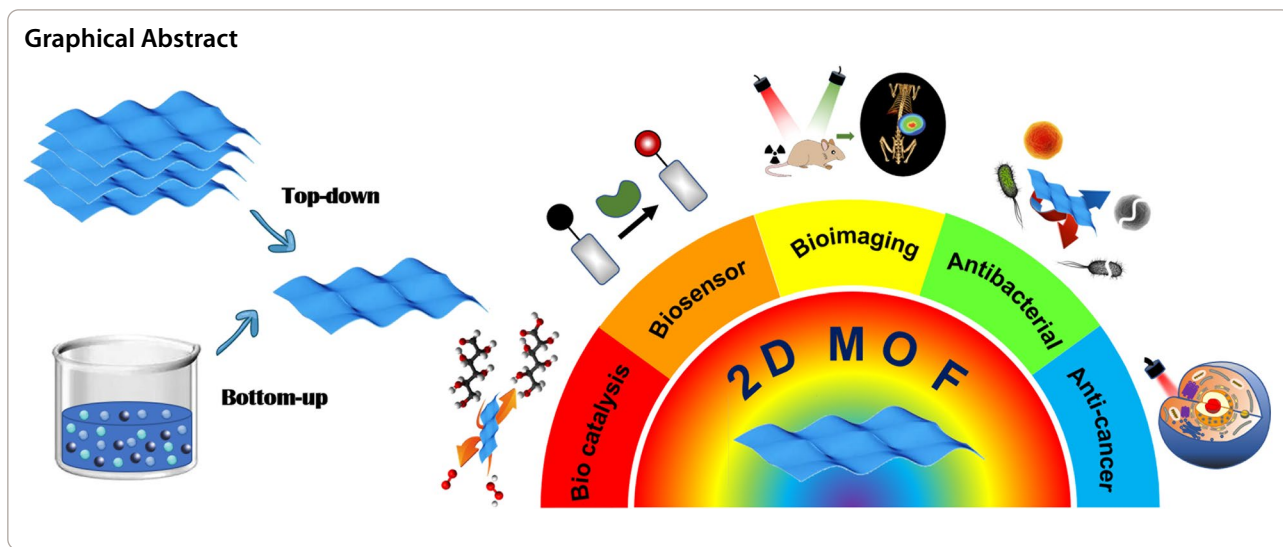
¹ School of Pharmacy, Nantong University, Nantong 226001, Jiangsu Province, China

² Department of Medical Imaging, Affiliated Hospital of Nantong University, Nantong 226001, Jiangsu Province, China

³ State Key Laboratory of Polymer Physics and Chemistry, Changchun Institute of Applied Chemistry, Chinese Academy of Sciences, Changchun 130022, China



© The Author(s) 2022. **Open Access** This article is licensed under a Creative Commons Attribution 4.0 International License, which permits use, sharing, adaptation, distribution and reproduction in any medium or format, as long as you give appropriate credit to the original author(s) and the source, provide a link to the Creative Commons licence, and indicate if changes were made. The images or other third party material in this article are included in the article's Creative Commons licence, unless indicated otherwise in a credit line to the material. If material is not included in the article's Creative Commons licence and your intended use is not permitted by statutory regulation or exceeds the permitted use, you will need to obtain permission directly from the copyright holder. To view a copy of this licence, visit <http://creativecommons.org/licenses/by/4.0/>. The Creative Commons Public Domain Dedication waiver (<http://creativecommons.org/publicdomain/zero/1.0/>) applies to the data made available in this article, unless otherwise stated in a credit line to the data.



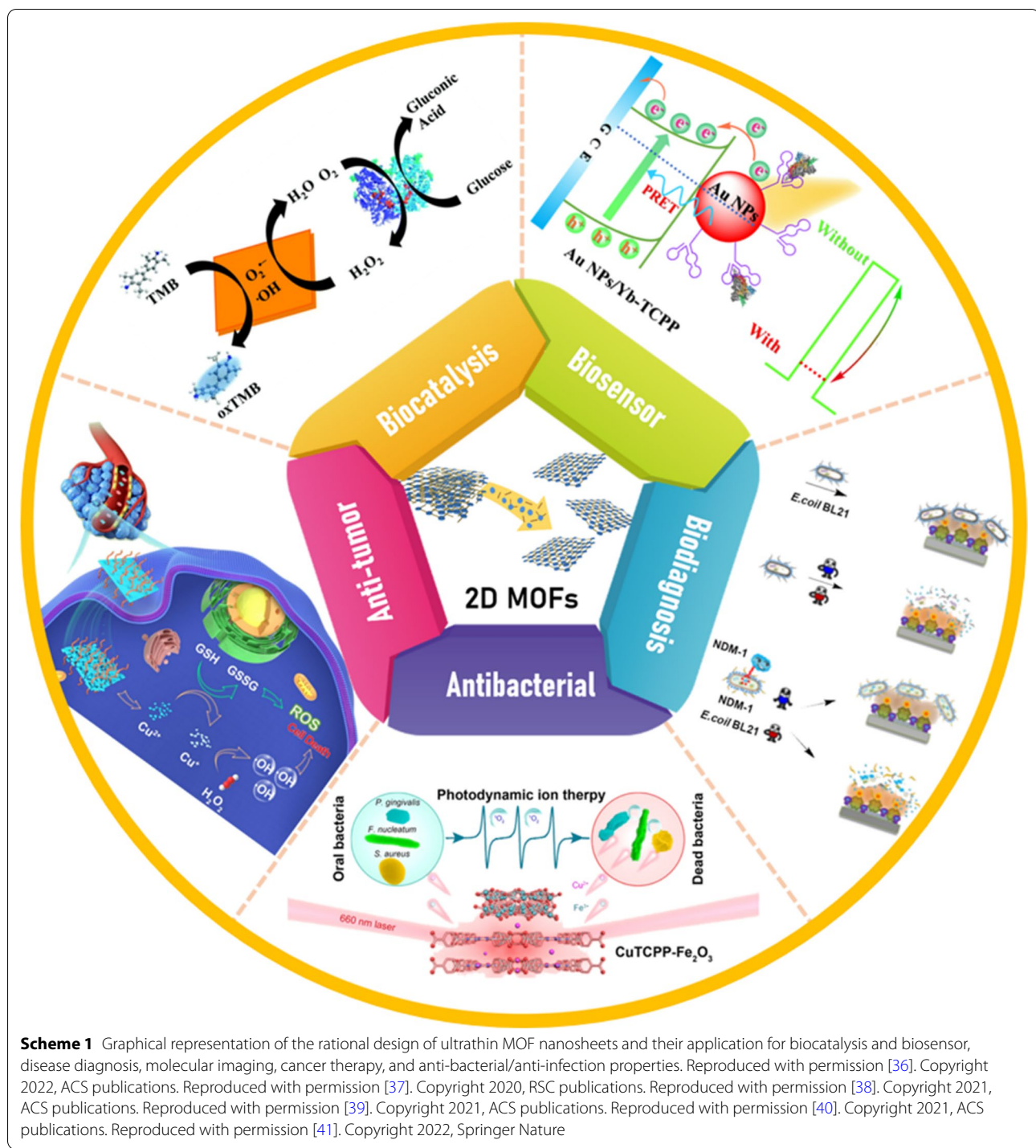
Introduction

As a rapidly developing class of hybrid materials, metal-organic frameworks (MOFs) [1] constructed by metal-ligand coordination into diverse supramolecular architectures encompass different dimensions. Compared to organic or inorganic materials, one typical advantage of well-defined supramolecular architectures is the tunable structure through nearly infinite metal ions or clusters bridged by polydentate organic linkers. Except for the compositional versatility, MOFs exhibit high surface-to-volume ratios, various topology, and flexible porosity. Moreover, the functionalization of MOFs would be easily obtained either by modification of the building blocks previously or post-modification of pre-synthesized MOFs. Owing to these outstanding features, MOFs have been widely applied in the field of gas storage [2] and separations [3, 4], nonlinear optics [5], catalysis [6, 7], and sensing [8, 9].

By choosing biologically friendly compositions, MOFs with good biocompatibility have been extensively investigated in the areas across biology and nanomedicine [10, 11]. For biomedical applications, the infinite array built from metal-ligand coordination endows the inherent biodegradability of MOFs under physiological conditions. Besides, the flexible porosity confers MOFs as candidates of nanocarriers for loading different types of active ingredients involving small molecules, peptides/proteins, or nucleic acids with high loading capacity [12, 13]. Furthermore, the unique optical and/or X-ray attenuation abilities of MOFs can be harnessed for molecular imaging, including fluorescence imaging, computed tomography [14], magnetic resonance imaging [15], and positron emission tomography [16]. For therapeutic applications, especially for

phototherapy or radiotherapy, photosensitizers and high-Z elements acting as organizing molecular building blocks integrated into the MOFs will augment reactive oxygen species (ROS) production [17, 18]. This desirable performance result from the enhanced inter-system crossing process and avoided aggregation of hydrophobic photosensitizers simultaneously. The two-dimensional MOFs (2D MOFs) are usually comprised of multiple ultrathin layers, possessing the characteristics of easy exposure of active sites and large surface area, which will embrace the great potential for various technological applications [19].

Similar to other 2D nanomaterials, the planar topography endows materials the intriguing physicochemical properties, including ductility, light transmittance, and electrical conductivity [20, 21]. Since the discovery of graphene in 2004 [22, 23], nanomaterials with high ratios of lateral size to thickness have been widely explored in biomedical applications. Up to date, 2D nanomaterials including transition metal dichalcogenides [24, 25], metal carbonitrides [26, 27], black phosphorus nanosheets [28, 29], layered double hydroxides [30, 31], MOFs, and covalent-organic frameworks [32] have aroused tremendous research attention in both synthetic methodology and/or practical applications. In particular, 2D MOFs displayed tailored structure, adjustable composition, efficient cargo loading, and good biodegradation, making these layered materials useful for biomedical applications [33]. Compared to the pristine MOFs, the ultrathin -nanosheet structures of 2D MOFs show distinct advantages for theranostic applications because of large surface areas, unique surface chemistry, and inherent optical properties derived from the fascinating topology. In particular, MOFs with



ultrathin layered structures allow for rapid diffusion of ROS, resulting in the elevated therapeutic performance of ROS-based treatment modalities.

So far, several systematic reviews have overviewed the synthetic methodology comprising the dimensional transformation, and their application in energy storage

and/or functional devices [34, 35]. Herein, we systematically summarized the latest advances of 2D MOFs applied in bio-related applications, especially for cancer theranostic applications (Scheme 1) [36–41]. First, we summarized the synthesis and surface modification

strategies of various types of 2D MOFs, focusing on structure–property relations. Then, we overviewed the most recent progress of multifunctional 2D MOFs in biomedical applications, including biocatalysis and biosensor, disease diagnosis, molecular imaging, malignancy management, and regenerative medicine. Emphasis is placed on the ROS-based treatment, involving photodynamic therapy (PDT) [42, 43], radioisotope therapy [44, 45], radiodynamic therapy (RDT) [46], chemodynamic therapy (CDT) [47, 48], and ROS-synergized cancer therapy. Finally, the existing challenges and outlooks in 2D MOFs are proposed based on the current development status and future requirements.

Synthetic methodology

The design strategy is of significant importance to control the dimensionality of nanomaterials. So far, the synthetic routes containing mechanical cleavage, liquid exfoliation, chemical vapor deposition, and wet chemistry, have been widely investigated [49–52]. Generally, strategies to construct 2DMOF materials have been classified into top-down and bottom-up approaches (Table 1) [53–60]. In the top-down strategy, namely the dimensional reduction strategy, harsh mechanical or chemical conditions are required for exfoliating the bulk materials into ultrathin nanosheets, such as mechanical shaking, ball milling, ultrasonic treatment, and insertion stripping [61]. Compared with the top-down method, the bottom-up approach is more flexible and designable to synthesize ultrathin nanomaterials by utilizing appropriate precursors. The bottom-up strategy, also known as bulk solution preparation, comprises interface synthesis, surfactant-assisted synthesis, and modulated synthesis, which has the advantages of easy control over the growth direction with a high yield.

Similar to the traditional synthetic strategy of 2D materials, several MOFs are suitable for exfoliation into ultrathin nanosheets while maintaining their crystallinity. So far, ultrasonic exfoliation is a general strategy for the exfoliation of bulk MOFs into MOF nanosheets by breaking the weak interactions between adjacent layers. For chemical exfoliation, pioneered work reported by Zhou et al. exploited chemically labile intercalating agent 4,4'-dipyridyl disulfide and trimethylphosphine to exfoliate crystalline MOFs ($Zn_2(PdTCPP)$) built from tetrakis(4-carboxyphenyl)porphyrin (TCPP) and Zn^{2+} to achieve single-layer nanosheets [53]. These nanofabrication techniques result in 2D MOFs with a highly uniform size distribution, however, MOF nanosheets isolated by exfoliation require harsh mechanical or chemical conditions. Meanwhile, the top-down exfoliation process requires extensive optimization and precise control, which usually leads to an extremely low yield. As a comparison, the direct assembly of metal ions and organic linkers through the bottom-up approach to fabricate MOF

nanosheets is more convenient. With the accessibility to the planar structure, the surfactant-assisted synthesis method gaining control over the crystallization process has shown great potential for practical application. As a paradigm, surfactant-assisted pre-organization of the metallic precursor was developed to synthesize NH_2 -MIL-53(Al) nanosheets, which is favored by the formation of oligomeric structures [62]. These MOF nanosheets exhibit a superior performance over other crystal morphologies in both chemical sensing and gas separation. In addition, exploiting monocarboxylic acids as “modulators”, He et al. have developed atomic thickness zirconium-porphyrinic MOF nanosheets with high-yield through one-pot solvothermal reaction [54]. Due to the planar topography, the 2D porphyrinic MOFs exhibited excellent-singlet oxygen generation capability and superior photocatalytic activity.

Apart from general synthetic considerations for 2D nanomaterials, engineering 2D MOFs synthetic routines involve a careful selection of organic spacer linkers with appropriate bridging groups to coordinate with metal ions/clusters with specific directionality [63]. Alternatively, the self-assembly of organic ligands and metal nodes enables the formation of MOFs with an atomic-layered structure during solution processing. To maximize the advantages of MOF nanosheets, the design strategy for the 2D MOFs is also concerned with the metal–ligand ratio, coordination number, coordination geometry, coordination environment, and structural transformation. Despite green synthesis and modification, the fabrication of large-scale 2D MOFs with high quality still faces huge challenges. The facile synthetic methodology is highly urgent to make these atomically ordered networks.

Bioapplications of 2D MOFs

Advancements in 2D MOFs for biomedical applications have occurred at a relatively slow pace compared with other 2D nanomaterials. With the diversity in the structural phases and the unique properties, the atomic-layered 2D MOFs have extraordinary advantages when exploited for various bioapplications [63, 64]. This section focused on the bioapplications of 2D MOFs for biocatalysis and biosensor, biological imaging, and theranostics.

Biocatalysis and biosensor

The selectivity towards target molecules is generally affected by the choice of the organic linkers and/or the metal ions that are introduced into the MOF structures. For example, different metal ions are usually accompanied by differentiated properties, such as magnetism, photoluminescence, as well as catalytic or sensing activity. As a comparison, MOF with sheet-like morphology confers their structure allows for more active site exposure for site-specific biocatalysis and biorecognition with

Table 1 The constituent composition, synthetic methodology, and physicochemical properties of porphyritic MOF nanosheets

Materials	2D MOFs		Methodology	Thickness (nm)	Refs.
	Metal	Ligand			
Zn ₂ (PdTCPP)	Zn(NO ₃) ₂ ·6H ₂ O		Intercalation and chemical exfoliation	~1	[53]
UNs-FA	ZrCl ₄		Solvothermal reaction	1.48±0.22	[54]
Zn-TCPP(Fe)	Zn ²⁺		Surface-assisted approach	1–1.5	[55]
Cu-TCPP(Fe)	Cu(NO ₃) ₂ ·3H ₂ O		Surfactant-assisted approach	3.5±1.2	[56]
M-TCPP(Fe)	Zn ²⁺ ; Co ²⁺ ; Cu ²⁺		Surfactant-assisted approach	–	[57]
PPF-Gd NS	Gd ³⁺		Surfactant-assisted approach	21.0±9.4	[58]
Fe-TBP	[Fe ₃ O(OAc) ₆ (H ₂ O) ₃]OAc		Solvothermal reaction	–	[59]
Hf-MOL	Hf ₁₂ (m ₃ -O) ₈ (m ₃ -OH) ₈ (m ₂ -OH) ₆		Solvothermal reaction	1.6	[60]

higher sensitivity. Concerning bioapplications, 2D MOFs have the potential to provide an efficient solution to the detection of heavy metals, medications, proteins, and exosomes (Table 2) [38, 65–69].

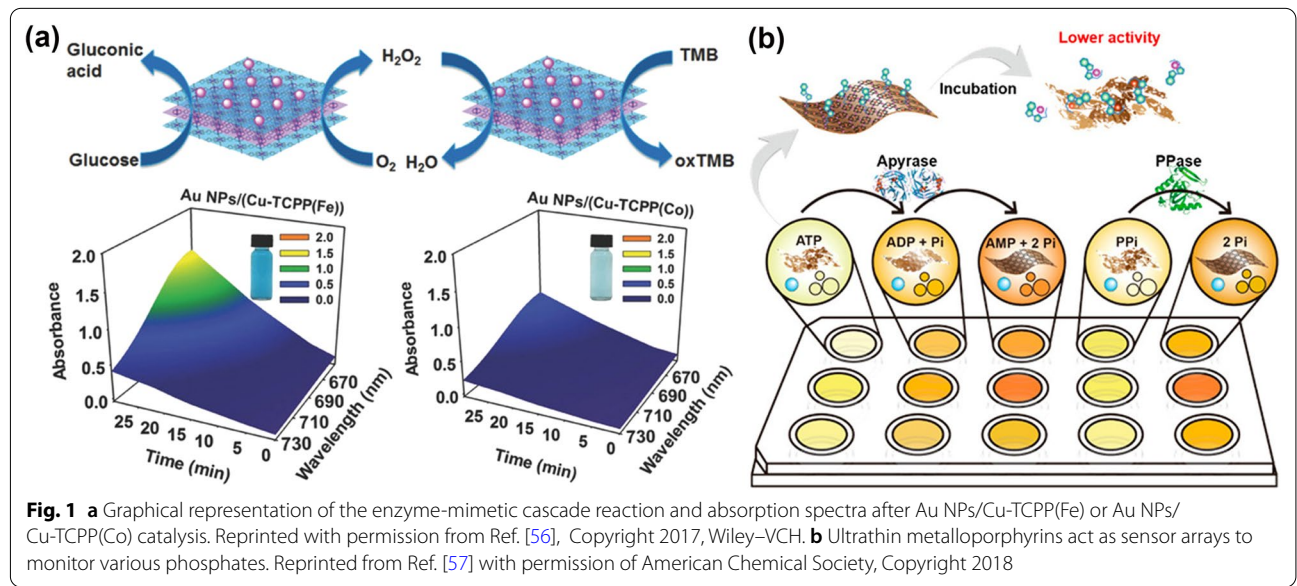
As an emerging nanoenzyme, MOFs with tunable structures and robust stability have aroused wide attention. Previous studies revealed that metalloporphyrins-based MOFs with layered topology exhibited an augmented peroxidase-mimicking activity when compared to their bulk analogs [67]. Employing the layered structure, Huang et al. designed and developed a nano-reactor (Au NPs/Cu-TCPP(Fe) or Au NPs/Cu-TCPP(Co)) to mimic the enzymatic cascade reactions [56]. A nano-biomimetic system was constructed by incorporating Au nanoparticles around 2.1 ± 0.5 nm onto the layered MOFs pre-synthesized by the surface-assisted method. In this biomimetic system, ultrasmall Au nanoparticles acting as glucose oxidase together with metalloporphyrins MOF nanosheets mimicking peroxidase facilitated the oxidation of 3,3',5,5'-tetramethylbenzidine and glucose simultaneously (Fig. 1a). As a proof of concept study, the absorbance at 652 nm for oxidation

of 3,3',5,5'-tetramethylbenzidine and the glucose concentrations displayed linear relationship ranges from 10×10^{-6} M to 300×10^{-6} M, and the colorimetric result can be identified by the naked eyes directly. More importantly, this study may open up a new avenue to design metalloporphyrins MOF-based nanosheets enabling biological catalysts with high catalytic activity, substrate specificity, and sustainability.

Due to the modular nature and unique surface, the layered MOFs with atomically precise structures have emerged as the prospective nanoplatforms for efficient catalysts within bioinspired systems. Given that, numerous approaches have been devoted to fabricating MOFs with a planar topography and the superior characteristics toward biocatalysis applications, including structural flexibility, required porosity, and inherent optical properties. Besides, MOFs with layered morphology is beneficial for minimizing the diffused barriers and maximizing the catalytic activity. The top-down synthesized MOF nanosheets were built from copper trifluoromethanesulfonate and 4,4-bipyridine [70]. The detection of hydrogen

Table 2 Representative porphyritic MOF nanosheets are used for the detection of biomarkers

2D MOFs	Biomarkers	Limitations	Sources	Refs.
Au NPs/Yb-TCPP	SARs-CoV2 spike glycoprotein	72 ng/mL	Throat swabs	[38]
Cu-TCPP(Fe)	Protein	0.742 pg/mL	Serum	[65]
Cu-TCPP	PD-L1 exosomes	16.7 particles/mL	Human serum	[66]
Cu-HHTP	Chemiresistive NH ₃	0.5 ppm	–	[67]
Yb-MOF	Picric acid and berberine chloride form	81.3 nM/36.5 nM	–	[68]
Cu-TCPP	Lead ions	3.3 nM	Tap water and fertilizer	[69]



peroxide and glucose was relied on converting non-fluorescent thiamine to strong fluorescent thiochrome in the presence of hydrogen peroxide. The selectivity and sensitivity of the biosensor were augmented when combined with glucose oxidase because of the supplement of hydrogen peroxide. The as-designed fluorescent biosensor with a low detection limit and wide ranges are established for clinical diagnosis indicators of glucose concentration in human serum. Mimicking the peroxidase, ultrathin metalloporphyrins MOFs were utilized to construct sensor arrays for the detection of phosphates and their enzymatic hydrolysis (Fig. 1b) [57]. Intriguingly, the selectivity of sensor arrays is originated from adjustable peroxidase-mimicking activity, which can give cross-reactive signals to discriminate multiple phosphates simultaneously. This work demonstrates a MOF-based nanoenzyme with tunable enzyme activity, providing a convenient and reliable analytical platform for practical application in biological samples.

Biodiagnosis

Compared to the bulk MOF crystals, 2D MOFs possess enhanced performance in catalysis and sensing application. These advantages are partly due to the ultrathin layer structures, which are capable of facilitating the exposure of the active site and the diffusion of the reactive matrix. Thereby, 2D MOFs with increased specificity towards biological entities have been employed for biological detections comprising glucose sensing, DNA discrimination, and detection of cancer biomarkers [71, 72]. Given the abundance of open sites on layered MOFs, pioneered work by the Lin group described the construction of layered MOFs (NA@Zr-BTB/F/R) and their application in the determination of mitochondrial dysregulation (Fig. 2a) [73]. The layered MOFs with Kagome topology built from $\{Zr_6\}$ cluster and 2,4,6-tris(4-carboxyphenyl) aniline ligands were modulated by formic acid through the solvothermal method. The monolayer Zr-BTB is about 1.5 ± 0.1 nm, which is consistent with the height of the formic acid connected $\{Zr_6\}$ cluster. Then, the active layer was afforded by postsynthetically modification with GSH-selective (2E)-1-(2'-naphthyl)-3-(4-carboxyphenyl)-2-propen-1-one (NA), pH-sensitive fluorescein isothiocyanate (FITC), and GSH/pH-independent rhodamine-B isothiocyanate (RITC). The fluorescent intensity along with GSH depletions and matrix acidification was reflected by the signals from FITC, RITC, and NA, respectively. As expected, the signals from FITC and RITC were constant, while NA signals increased with the variation of GSH concentrations. In parallel, the constant signals of NA and RITC change signals obviously of FITC when the solution pH changes, which is agreed with the results at the cellular

level. More importantly, there is a good linear correlation between the ratiometric fluorescent intensity and the GSH concentrations and pH variations. Mitochondrial dysfunction impacts GSH consumption and hydrogen ion effluxing, which has been implicated in diseases chemoresistance cancers. Thereafter, the layered MOFs enabling ratiometric fluorescent detection for GSH concentrations and pH values have pinpointed the role of mitochondrial DNA alterations on the onset of chemoresistance with extensively practical applications.

Recently, the emergence of antibiotic-resistant bacteria [74, 75] has underscored the urgent need for rapid testing technologies of antimicrobial susceptibility. Thereby, suitable antibiotics could be prescribed in order to provide effective therapeutic options. In comparison with the time-consuming determination, the biosensor can be a suitable strategy for susceptibility testing. Based on this ground, 2D MOFs assisted electrochemiluminescence biosensors (Ru-Con A@NH₂-MIL-53(Al)) was developed for the detection of Gram-negative bacteria and antimicrobial susceptibility (Fig. 2b) [39]. The electrogenerated chemiluminescence (ECL) biosensor comprised three components, involving recognition molecule concanavalin A, electrode-modified material NH₂-MIL-53(Al) nanoplate, and ECL probe ruthenium(II) complex. The ECL signals decreased in proportional to the increasing concentrations of *Escherichia coli* (*E. coli*) BL21, owing to the specific recognition by concanavalin A modified MOF material. Strikingly, the detection limit reached up to 16 cells/mL, which is even lower than the CRISPR-Cas9-triggered fluorescence signals amplification. Besides, the Ru-Con A@NH₂-MIL-53(Al) with excellent sensitivity, selectivity, and stability was also suitable for rapid detection of antimicrobial susceptibility, which may facilitate antibiotic stewardship in the clinical application.

Molecular imaging

Molecular imaging with non-invasive characteristics is an important methodology for the identification of disease progression [76, 77]. Contrast agents with good biological imaging performance are urgently needed to meet the requirements in clinical settings [78, 79]. Especially, the resolution of imaging in cancer diagnostics is important for real-time guidance of surgical resection, as well as the early detection of tumors. Fluorescence imaging with high spatial resolutions is an indispensable tool for cancer diagnosis in preclinical research [80, 81]. Biodegradable MOF nanosystems (DNA@Cu-MOF) integrated DNAzyme-assisted fluorescence signal amplification was applied for imaging deregulated miRNA-related hypoxic tumors [82]. In their structure design, the hypoxia-responsive Cu-MOFs were constructed by the

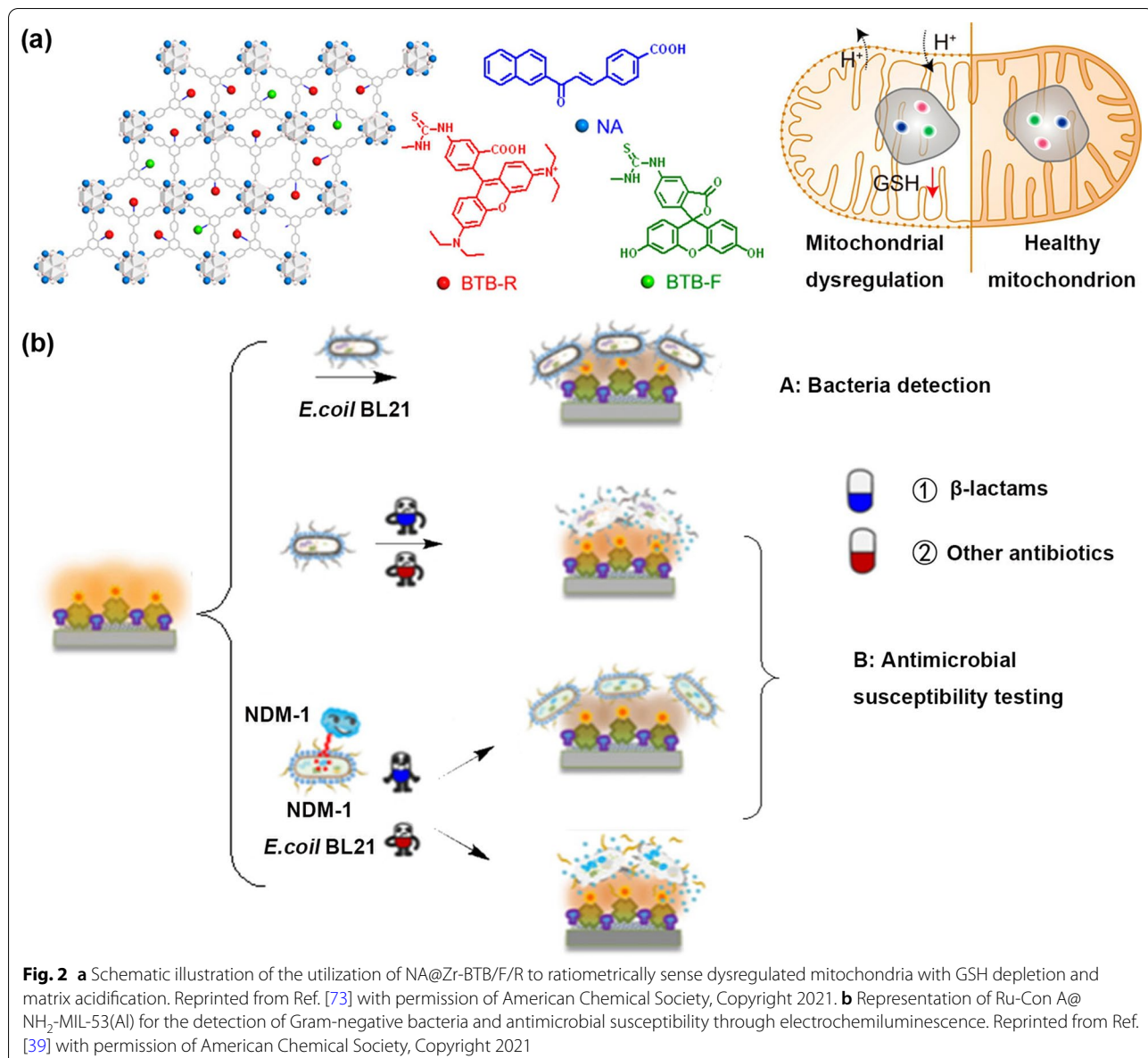
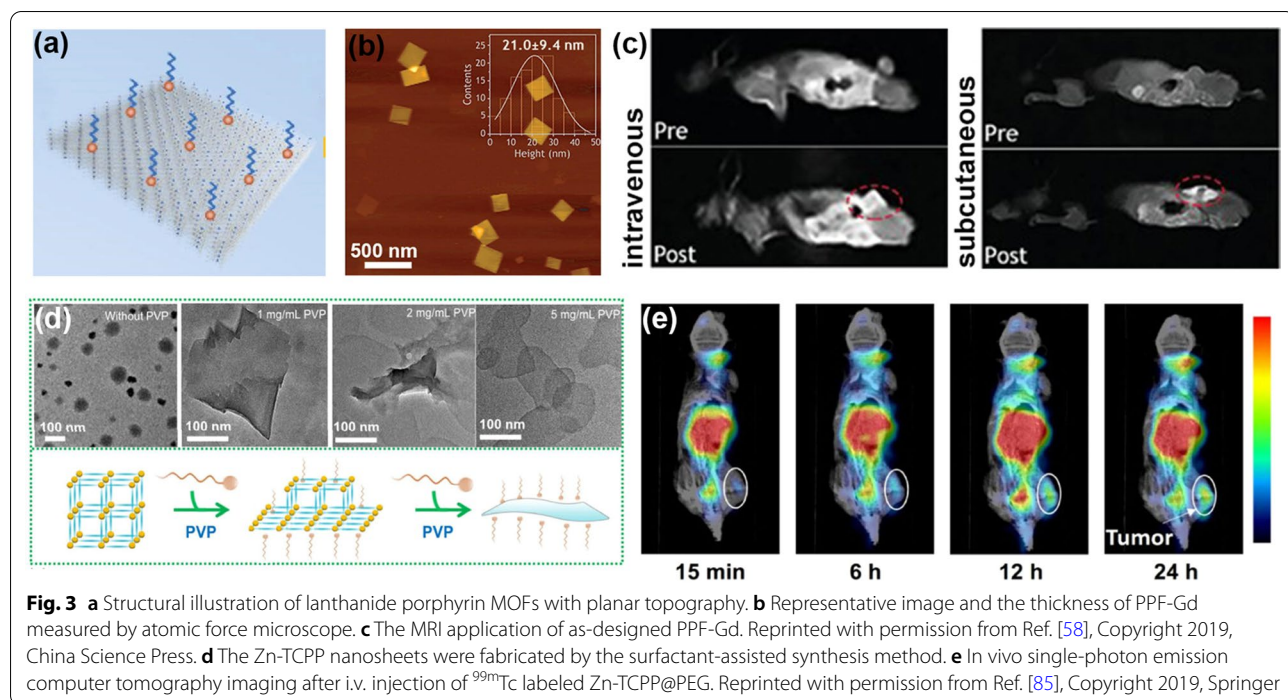


Fig. 2 **a** Schematic illustration of the utilization of NA@Zr-BTB/F/R to ratiometrically sense dysregulated mitochondria with GSH depletion and matrix acidification. Reprinted from Ref. [73] with permission of American Chemical Society, Copyright 2021. **b** Representation of Ru-Con A@ $\text{NH}_2\text{-MIL-53(Al)}$ for the detection of Gram-negative bacteria and antimicrobial susceptibility testing through electrochemiluminescence. Reprinted from Ref. [39] with permission of American Chemical Society, Copyright 2021

surfactant-assisted solvothermal method. When encountering the low oxygen environment in solid tumors, the MOFs degraded and released the loaded Cu-specific DNAzyme precursor. The DNAzyme precursor displaced by the aberrant miRNA resulted in the recovery of fluorescence signals in an expression-dependent manner. Noteworthy, the hypoxia and miRNA are readily applied for initiating sustained signal amplification, fulfilling the requirements for the temporal and spatial detection *in vivo*.

However, single imaging modalities often fail to collect reliable clinical information. Currently, combining multiple imaging modalities is more desirable for practical

applications [83, 84]. A MOF bridged by porphyrin derivatives and lanthanide elements exhibits outstanding magnetic and luminescent properties, thereby making them promising candidates for diagnostic applications. In this aspect, Xia et al. designed and developed a series of lanthanide porphyrin MOFs (PPF-Ln, Ln = Ce, Eu, Gd, Tb, and Ho) with a surfactant-assisted wet chemistry strategy (Fig. 3a) [58]. The gadolinium-based porphyrin framework (PPF-Gd) integrated TCPP and lanthanide element Gd. The PPF-Gd with a thickness of 21.0 ± 9.4 nm exhibits excellent photoluminescence properties and magnetic resonance imaging capability (Fig. 3b, c). Interestingly, the PPF-Gd exhibited negligible side effects



and a biodegradation profile in response to intratumoral acidity. This work further supports the great potential of MOF-based systems with deep tumor penetration and controllable biodegradability, which may broaden the practical application of bimodal imaging technology.

To improve the colloidal stability and biocompatibility, porphyrin-based MOF nanosheets utilizing Zn^{2+} as connecting metal ions were synthesized, and surface modified with polyethylene glycol (PEG) (Fig. 3d) [85]. Interestingly, the as-designed MOF nanosheets are easily labeled with gamma emission radioisotope $^{99\text{m}}\text{Tc}$ by simple mixing. Thereby, the $^{99\text{m}}\text{Tc}$ labeled Zn-TCPP@PEG possesses enormous potential for in vivo single-photon emission computer tomography imaging (Fig. 3e). For 4T1-bearing mice, the $^{99\text{m}}\text{Tc}$ labeled Zn-TCPP@PEG displayed a high degree of tumor homologous ability, and the results were agreed well with the quantification of Zn according to inductively coupled plasma spectrometry. Moreover, these 2D MOFs exhibited indiscernible long-term toxicity, demonstrating the great potential of biodegradable multifunctional nanoplateform for theranostic applications.

Biomedicine

The porosity MOFs with planar topology provided high surface-to-area, abundance active sites, easily surface modification for applications across biology and medicine, including 3D printing [86, 87], tissue engineering [88, 89], wound healing [90, 91], inflammatory disease

[92, 93], or cancer treatment [94, 95]. In this section, recent progress of layered MOFs in antibacterial and/or antitumor application was overviewed, with an emphasis on ROS-based treatment.

Antibacterial application

Chronic diabetic wounds suffer from unexpected epithelium injuries because of the inability to spontaneously heal and vulnerability to bacterial infection [96, 97]. Efficient strategies to promote injury recovery require angiogenesis promotion, collagen deposition, and re-epithelialization simultaneously to combat chronic non-healing wounds. The emergence of nanotechnology has facilitated wound closure and addressed pathophysiological abnormalities in patients with diabetes. For example, copper-based MOFs (HKUST-1) displayed improved wound closure by modulating the release of copper ions to stimulate angiogenesis and collagen deposition [98]. Compared with three-dimensional bulk MOFs, 2D MOFs exhibited superior enzymatic catalysis activity due to their unique topological structure. Thereby, ultrathin MOF (Cu-TCPP(Fe)) with superior peroxidase-mimic activity was selected to construct a self-activated cascade nanoreactor for promoting in vivo wound closure (Fig. 4a) [99]. Glucose oxidase (GOx) was physically adsorbed onto Cu-TCPP(Fe) nanosheets, demonstrating the efficient conversion of glucose into gluconic acid and H_2O_2 . The generated gluconic acid and H_2O_2 decreased the environmental pH and offered sufficient substrates,

which synergistically activated the peroxidase-like activity of Cu-TCPP(Fe) nanosheets. Overall, the hydroxyl radical generated from MOF-based hybrid nanocatalyst possesses a robust antibacterial effect and negligible damage to normal tissues.

Similarly, ferric oxide-modified porphyrinic MOF layers (Cu-TCPP/Fe₂O₃) were employed to treat chronic diseases like periodontitis (Fig. 4b) [40]. The hybrid nanosheets constructed by atomic layer deposition (ALD) were incorporated into a poly(ethylene glycol) matrix to form a photoresponsive ointment. As schematically illustrated, this surface-engineered MOF heterojunction induced efficient killing towards diverse oral pathogens through synergistic ROS production induced by PDT and ion intervention. According to the theoretical calculation, the metal-connected MOF structure facilitated charge transfer and improved light-harvesting capacity, leading to enhanced photocatalytic activity. As a comparison, the photodynamic ion therapy triggered by ALD-engineered MOFs shows a better antimicrobial effect than the clinical antibiotic treatment, like minocycline and vancomycin. These MOF layers exhibit broad-spectrum antimicrobial activity, which may provide a universal synthetic method to optimize periodontitis treatment by reducing inflammation and promoting angiogenesis.

Cancer treatment

MOF structures possess the advantages of a variety of organic linkers/inorganic built units, infinite arrangements, fine-tuning potential. Compared to the pristine 3D MOF, MOFs with sheet-like morphologies confers their larger surface area, higher flexibility, and more exposed active sites. Owing to these unique features, 2D MOFs are increasingly used in the drug delivery system, especially for oncology treatment (Table 3) [100–106]. Concerning pharmaceutical applications, 2D MOFs often exhibit high drug upload capacity towards various active pharmaceutical ingredients, including chemotherapeutics, antigens, antibodies, and immuno-adjuvants. Besides, active pharmaceutical ingredients loaded by planar MOF enable overcoming issues associated with stability, solubility, and systematic cytotoxicity. For example, leaf-shaped MOF (NZIF-L) through rapid scale-up synthesis have been employed for co-delivery of chemotherapeutic DOX and imaging agents

4,4'-(1,2-diphenylvinyl)-1,2-di-(phenyl carboxylic acid) (TCPE) [100].

MOFs with planar topology possess their unique superiority in ROS generation by nanocatalytic medicine [107, 108]. Generally, the precisely arranged framework enables the diffusion of ROS and molecular oxygen. At the same time, photosensitizers serve as the building block of MOFs that can effectively avoid self-quenching. Pioneered work by Lin's group has reported a series of layered MOF structures with enhanced PDT performance constructed from 5,10,15,20-tetra(*p*-benzoato) porphyrin (TBP) [102, 105], 5,10,15,20-tetra(*p*-benzoato) chlorin (TBC) [106], and 5,10,15,20-tetra(*p*-benzoato) bacteriochlorin (TBB) [109]. To potentiate PDT efficacy, iron-oxo clusters-based MOFs (Fe-TBP) were developed to overcome tumor hypoxia by decomposition of endogenous H₂O₂ (Fig. 5) [59]. As evidenced by immunofluorescence, the immunogenic PDT elicited by Fe-TBP dramatically improved the calreticulin (CRT) exposure (Fig. 5b). Moreover, the Fe-TBP mediated PDT is capable of elevating the object response of anti-programmed death-ligand 1 (α-PD-L1) treatment. In the colorectal tumor model, necrotic tumor histology was observed after Fe-TBP + α-PD-L1 treatment, demonstrating that the combinatory treatment elicited obvious abscopal effects. The Fe-TBP plus α-PD-L1 group showed a significant increase of tumor-infiltrating CD4⁺ and CD8⁺ T cells in both primary and distant tumors (Fig. 5c). In turn, the immunotherapeutic efficacy was comprised by depletion of either B cells or CD4⁺ or CD8⁺ T cells (Fig. 5d, e). Overall, this study presents a general strategy to alleviate hypoxia in solid tumors for PDT primed immunotherapy of colorectal carcinoma.

Despite being approved by Food and Drug Administration, the clinical application of PDT in solid tumors is still limited to superficial malignant lesions. Radiotherapy (RT) overcomes the limitations of tissue penetration but suffers from radioresistance and unwanted side effects [110]. Many innovative kinds of research have been devoted to developing radio enhancers for addressing the safety issues accompanied by using low-dose X-rays [111]. As a paradigm, Ni et al. designed and developed an ultrathin MOF layer (Hf-MOL) for radiotherapeutic enhancement (Fig. 6) [60]. The as-designed Hf-MOL was synthesized by the solvothermal reaction from HfCl₄ and DBP with acetic acid as modulators.

(See figure on next page.)

Fig. 4 **a** Illustration of the self-activated cascade reaction catalytic by MOF/GOx hybrid nanosheets. Scanning electron microscopic observation of *E. coli* and *S. aureus* after indicated treatment. 1: PBS, 2: glucose, 3: glucose + MOF, 4: MOF/GOx, 5: glucose + GOx, 6: glucose + MOF/GOx, respectively. Reprinted from Ref. [99] with permission of American Chemical Society, Copyright 2019. **b** Carton representation of the antibacterial mechanism of Cu-TCPP/Fe₂O₃ mediated photodynamic ion therapy. **c** Histological analysis of periodontium stained by hematoxylin and eosin (H&E), Masson's trichrome, vascular endothelial growth factor (VEGF), and CD31. Scale bars represent 500 μm for low-magnification, while 50 μm for high-magnification and immunohistochemical images. Reprinted from Ref. [40] with permission of American Chemical Society, Copyright 2021

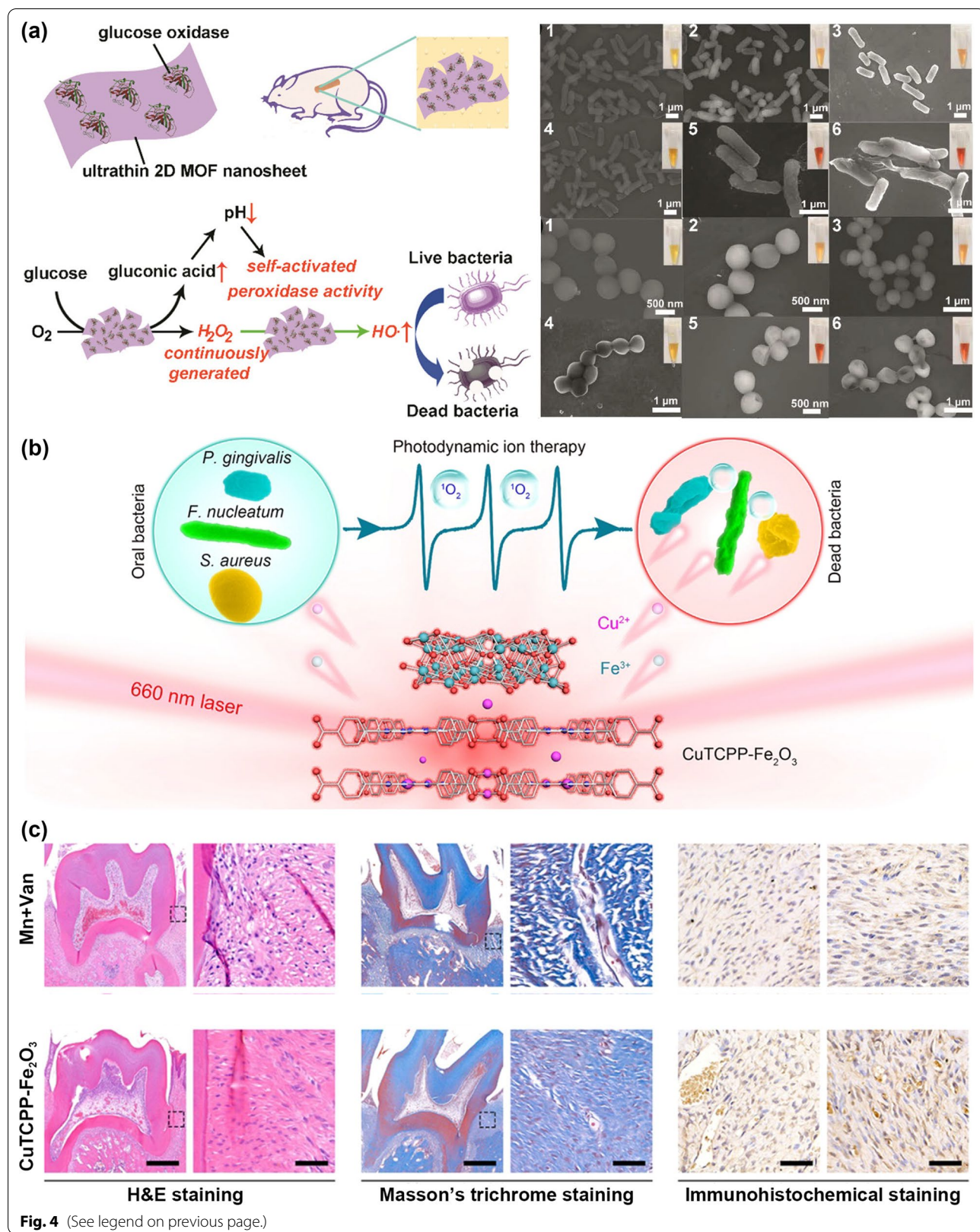


Table 3 Recent breakthroughs associated with 2D MOFs for oncology treatment

2D MOFs	Therapeutics	Drug loading	Treatment	Cells/animals	Refs.
NZIF-L	DOX	~ 3.5 wt% for DOX ^a	Chemotherapy	HeLa cells	[100]
PPF	SOR	84% for SPR ^b	Molecular targeted therapy	McA RH7777-bearing rats (Subcutaneous)	[101]
Ti-TBP	TBP	–	Type I PDT	CT26-bearing BALB/c mice (Subcutaneous)	[102]
Cu-TCPP	Cu ²⁺ , TCPP, and DOX	33% for DOX ^b	Chemotherapy/PDT/GSH consumption	4T1 bearing nude mice (Groin)	[103]
Gd-TCPP	Gd ³⁺ , TCPP, and NC-FAA	–	MRI/SDT/Starvation therapy/GSH consumption	A498 bearing mice (Subcutaneous)	[104]
W-TBP	TBP, CpG, and αPD-L1	87.9% for CpG ^b	PDT/Adjuvant/ICB	TUBO bearing mice (Bilateral subcutaneous)	[105]
Hf-TBC	TBC, and IDO ⁱ	4.7 wt% for IDO ⁱ ^a	PDT/ICB	MC38 bearing mice (Bilateral subcutaneous)	[106]

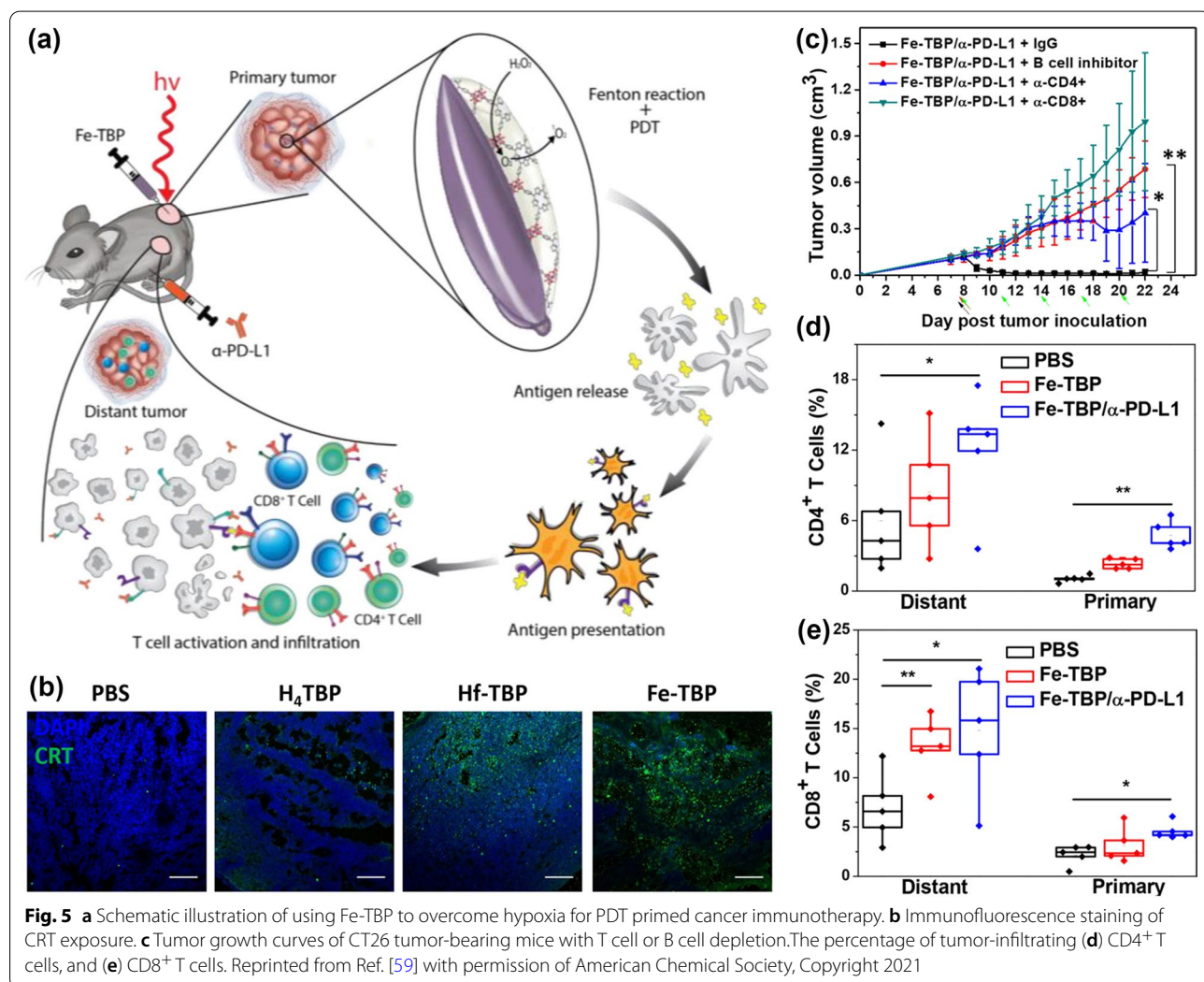
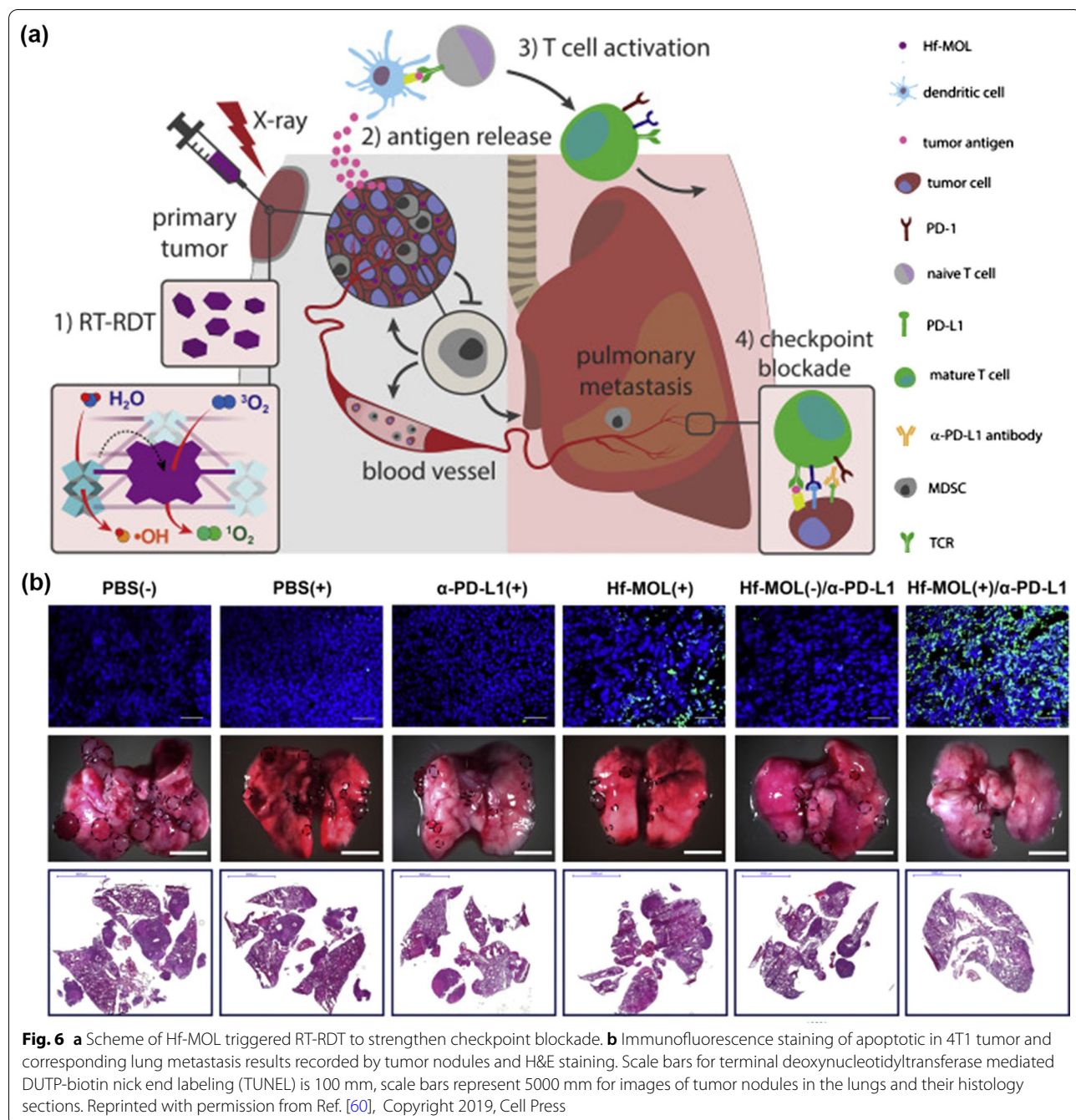
^a Drug loading efficiency^b Drug loading capacity

Fig. 5 **a** Schematic illustration of using Fe-TBP to overcome hypoxia for PDT primed cancer immunotherapy. **b** Immunofluorescence staining of CRT exposure. **c** Tumor growth curves of CT26 tumor-bearing mice with T cell or B cell depletion. The percentage of tumor-infiltrating **(d)** CD4⁺ T cells, and **(e)** CD8⁺ T cells. Reprinted from Ref. [59] with permission of American Chemical Society, Copyright 2021

Owing to the reduced dimensionality, Hf-MOL allows rapid diffusion of ROS/O₂. In the orthotopic breast cancer model, RT-RDT treatment exhibited a superior

tumor regression effect even at a radiation dose as low as 1 Gy/fraction. Combination with α-PD-L1 this innovative platform resulted in remarkable antimetastatic



effects in histological examination (Fig. 6b), which can be explained by reactivating antitumor immunity and reversing tumor immunosuppression. In addition, this synergy treatment also elicited robust abscopal effects in bilateral colorectal carcinoma, head and neck cancer, and breast cancers, demonstrating a generalized strategy for radioimmunotherapy of advanced malignancies.

Conclusion and prospect

At present, 2D-MOF materials integrate ultrathin thickness, large surface-to-volume ratio, variety of ligands, permanent porous structure, and highly designability, which has steadily exhibited great potential in nanomedicine and biology. With the development of new nanofabrication technologies, ultrathin MOF nanosheets with desired features will be brought to the forefront of advanced materials to broaden their fundamental and

preclinical investigations. Despite remarkable achievements that have been made in the bioapplications of 2D MOFs, this research is still in its primary stage. Shortcomings and deficiencies originating from 2D MOFs, such as the physiological stability and long-term toxicity, continuous industrial production, precise control of lateral size, and lack of innovative applications, still need to be addressed. Even though preliminary research involving 2D MOFs has expanded rapidly, the utilization of 2D MOFs for biomedical applications is approached with cautious optimism owing to the lack of comprehensive material characterization and toxicological studies, especially for those involving long-term administration. Meanwhile, the toxicity of 2D MOFs relies on the synthetic/processing process accompanied by changes in the material composition and degradation characteristics, making it difficult to precisely assess the hazard potential of 2D MOFs. To promote industrial production, considerable efforts were devoted to developing efficacious nanofabrication strategies, integration of emerging technologies such as surface acoustic wave assisted exfoliation, high-throughput droplet microfluidic synthesis, and surfactant-free and scalable general strategy. Furthermore, 2D MOF design should also be focused on the prospect in crystal dissolution-growth kinetics, topotactic transformation, machine-learning for guiding synthetic mythology and control over morphology. Besides, the synthesis in large-scale, high-quality 2D MOFs with superior optical, electrical and magnetic properties is still lacking. In terms of the atomically layered MOF structures, it is necessary to broaden the exploration and promote scientific developments.

In the next generation of nanotechnology, 2D MOFs with more flexibility and tunability should be focused on the development requirements towards wearable devices, 3D printing, and artificial intelligence. Taking the advantage of the flexibility derived from the planar topography, ultrathin MOF nanosheets are ideal alternatives to fabricate wearable and implantable devices for autonomous monitoring of physiological markers. Moreover, it is profoundly meaningful to construct composite materials combining the advantages of each module, thus obtaining hybrid materials with good application prospects, such as transplantable artificial tissues, photosynthetic artificial organelles, and other medical equipment. Overall, the 2D MOFs with high performance and high integration will have good prospects as technologically indispensable materials in the future.

Abbreviations

MOFs: Metal-organic frameworks; ROS: Reactive oxygen species; PDT: Photodynamic therapy; RDT: Radiodynamic therapy; CDT: Chemodynamic therapy; TPP: Tetrakis(4-carboxyphenyl)porphyrin; FITC: Fluorescein isothiocyanate;

RITC: Rhodamine-B isothiocyanate; ECL: Electrogenerated chemiluminescence; PEG: Polyethylene glycol; Gox: Glucose oxidase; HKUST-1: Copper-based MOFs; ALD: Atomic layer deposition; H&E: Hematoxylin and eosin; VEGF: Vascular endothelial growth factor; NZIF-L: Leaf-shaped MOF; TCPE: 4,4'-(1,2-Diphenylvinyl)-1,2-di-(phenyl carboxylic acid); TBP: Tetra(*p*-benzoato)porphyrin; TBC: Tetra(*p*-benzoato)chlorin; TBB: Tetra(*p*-benzoato)bacteriochlorin; CRT: Calreticulin; α-PD-L1: Anti-programmed death-ligand 1; RT: Radiotherapy; TUNEL: DUTP-biotin nick end labeling.

Acknowledgements

Financial support from the National Natural Science Foundation of China (52103169, 31900990 and 51973214), and the Nantong Municipal Science and Technology Project (JCZ19090) are gratefully acknowledged.

Author contributions

WW: Conceptualization and writing-original draft. YY: Processing the pictures and copyright permission. YJ: Writing Part of the original draft. XL: Revised part of the draft. MS: Revised part of the draft. XZ: Review and support the foundation. TL: Review and support the foundation. ZX: Supervision and foundation. All authors read and approved the final version of the manuscript.

Funding

This work was supported by the National Natural Science Foundation of China (Project NO. 52103169, 31900990, and 51973214), and the Nantong Municipal Science and Technology Project (Project NO. JCZ19090).

Availability of data and materials

Yes.

Declarations

Ethics approval and consent to participate

Yes.

Consent for publication

Yes.

Competing interests

The authors declare that they have no competing financial interests or personal relationships that could have appeared to influence the work reported in this paper.

Received: 20 January 2022 Accepted: 23 March 2022

Published online: 02 May 2022

References

1. Furukawa H, Cordova Kyle E, O'Keeffe M, Yaghi OM. The chemistry and applications of metal-organic frameworks. *Science*. 2013;341:1230444.
2. Chen Z, Mian MR, Lee SJ, Chen H, Zhang X, Kirlikovali KO, Shulda S, Melix P, Rosen AS, Parilla PA, et al. Fine-tuning a robust metal-organic framework toward enhanced clean energy gas storage. *J Am Chem Soc*. 2021;143:18838–43.
3. Zhao X, Wang Y, Li DS, Bu X, Feng P. Metal-organic frameworks for separation. *Adv Mater*. 2018;30:e1705189.
4. Pei J, Wen HM, Gu XW, Qian QL, Yang Y, Cui Y, Li B, Chen B, Qian G. Dense packing of acetylene in a stable and low-cost metal-organic framework for efficient C_2H_2/CO_2 separation. *Angew Chem Int Ed*. 2021;60:25068–74.
5. Li D, Li Q, Wang Z, Ma Z, Gu Z, Zhang J. Interpenetrated metal-porphyrinic framework for enhanced nonlinear optical limiting. *J Am Chem Soc*. 2021;143:17162–9.
6. Shen Y, Pan T, Wang L, Ren Z, Zhang W, Huo F. Programmable logic in metal-organic frameworks for catalysis. *Adv Mater*. 2021;33:e2007442.
7. Li J, Liao J, Ren Y, Liu C, Yue C, Lu J, Jiang H. Palladium catalysis for aerobic oxidation systems using robust metal-organic framework. *Angew Chem Int Ed*. 2019;58:17148–52.
8. Li S, Hu X, Chen Q, Zhang X, Chai H, Huang Y. Introducing bifunctional metal-organic frameworks to the construction of novel ratiometric

- fluorescence sensor for screening acid phosphatase activity. *Biosens Bioelectron.* 2019;137:133–9.
9. Wu S, Sun Z, Peng Y, Han Y, Li J, Zhu S, Yin Y, Li G. Peptide-functionalized, metal–organic framework nanocomposite for ultrasensitive detection of secreted protein acidic and rich in cysteine with practical application. *Biosens Bioelectron.* 2020;169:112613.
 10. Simon-Yarza T, Mielcarek A, Couvreur P, Serre C. Nanoparticles of metal–organic frameworks: on the road to *in vivo* efficacy in biomedicine. *Adv Mater.* 2018;30:e1707365.
 11. Xiang X, Pang H, Ma T, Du F, Li L, Huang J, Ma L, Qiu L. Ultrasound targeted microbubble destruction combined with Fe-MOF based bio-/enzyme-mimics nanoparticles for treating of cancer. *J Nanobiotechnol.* 2021;19:92.
 12. Sun Y, Zheng L, Yang Y, Qian X, Fu T, Li X, Yang Z, Yan H, Cui C, Tan W. Metal–organic framework nanocarriers for drug delivery in biomedical applications. *Nanomicro Lett.* 2020;12:103.
 13. Huang R, Cai G, Li J, Li X, Liu H, Shang X, Zhou J, Nie X, Gui R. Platelet membrane-camouflaged silver metal–organic framework drug system against infections caused by methicillin-resistant *Staphylococcus Aureus*. *J Nanobiotechnol.* 2021;19:229.
 14. Zhang T, Wang L, Ma C, Wang W, Ding J, Liu S, Zhang X, Xie Z. BODIPY-containing nanoscale metal–organic frameworks as contrast agents for computed tomography. *J Mater Chem B.* 2017;5:2330–6.
 15. Yang Y, Zhang Y, Wang B, Guo Q, Yuan Y, Jiang W, Shi L, Yang M, Chen S, Lou X, Zhou X. Coloring ultrasensitive MRI with tunable metal–organic frameworks. *Chem Sci.* 2021;12:4300–8.
 16. Chen D, Yang D, Dougherty CA, Lu W, Wu H, He X, Cai T, Van Dort ME, Ross BD, Hong H. In vivo targeting and positron emission tomography imaging of tumor with intrinsically radioactive metal–organic frameworks nanomaterials. *ACS Nano.* 2017;11:4315–27.
 17. Zheng X, Jin Y, Liu X, Liu T, Wang W, Yu H. Photoactivatable nano-generators of reactive species for cancer therapy. *Bioact Mater.* 2021;6:4301–18.
 18. Lan G, Ni K, Lin W. Nanoscale metal–organic frameworks for phototherapy of cancer. *Coord Chem Rev.* 2019;379:65–81.
 19. Lin Y, Li Y, Cao Y, Wang X. Two-dimensional MOFs: design & synthesis and applications. *Chem Asian J.* 2021;16:3281–98.
 20. Liu S, Pan X, Liu H. Two-dimensional nanomaterials for photothermal therapy. *Angew Chem Int Ed.* 2020;59:5890–900.
 21. Murali A, Lokhande G, Deo KA, Brokesh A, Gaharwar AK. Emerging 2D nanomaterials for biomedical applications. *Mater Today.* 2021;50:276–302.
 22. Novoselov KS, Geim AK, Morozov SV, Jiang D, Zhang Y, Dubonos SV, Grigorieva IV, Firsov AA. Electric field effect in atomically thin carbon films. *Science.* 2004;306:666–9.
 23. Wang X, Hu C, Gu Z, Dai L. Understanding of catalytic ROS generation from defect-rich graphene quantum-dots for therapeutic effects in tumor microenvironment. *J Nanobiotechnol.* 2021;19:340.
 24. Huang H, Zha J, Li S, Tan C. Two-dimensional alloyed transition metal dichalcogenide nanosheets: synthesis and applications. *Chin Chem Lett.* 2022;33:163–76.
 25. Yang W, Huang T, He J, Zhang S, Yang Y, Liu W, Ge X, Zhang R, Qiu M, Sang Y, et al. Monolayer WS₂ lateral homosuperlattices with two-dimensional periodic localized photoluminescence. *ACS Nano.* 2022;16:597–603.
 26. Szuplewska A, Kulpinska D, Dybko A, Chudy M, Jastrzebska AM, Olszyna A, Brzozka Z. Future applications of MXenes in biotechnology, nanomedicine, and sensors. *Trends Biotechnol.* 2020;38:264–79.
 27. Zhu X, Zhang Y, Liu M, Liu Y. 2D titanium carbide MXenes as emerging optical biosensing platforms. *Biosens Bioelectron.* 2021;171:112730.
 28. Wang Z, Liu Z, Su C, Yang B, Fei X, Li Y, Hou Y, Zhao H, Guo Y, Zhuang Z, et al. Biodegradable black phosphorus-based nanomaterials in biomedicine: theranostic applications. *Curr Med Chem.* 2019;26:1788–805.
 29. Deng X, Liu H, Xu Y, Chan L, Xie J, Xiong Z, Tang Z, Yang F, Chen T. Designing highly stable ferrous selenide-black phosphorus nanosheets heterostructure via P-Se bond for MRI-guided photothermal therapy. *J Nanobiotechnol.* 2021;19:201.
 30. Duan M, Liu S, Jiang Q, Guo X, Zhang J, Xiong S. Recent progress on preparation and applications of layered double hydroxides. *Chin Chem Lett.* 2021. <https://doi.org/10.1016/j.ccl.2021.12.033>.
 31. Zhao J, Wu H, Zhao J, Yin Y, Zhang Z, Wang S, Lin K. 2D LDH-MoS₂ clay nanosheets: synthesis, catalase-mimic capacity, and imaging-guided tumor photo-therapy. *J Nanobiotechnol.* 2021;19:36.
 32. Li C, Yu G. Controllable synthesis and performance modulation of 2D covalent-organic frameworks. *Small.* 2021;17:e2100918.
 33. ArunKumar S, Balasubramaniam B, Bhunia S, Jaiswal MK, Verma K, Prateek, Khademhosseini A, Gupta RK, Gaharwar AK. Two-dimensional metal–organic frameworks for biomedical applications. *Wiley Interdiscip Rev Nanomed Nanobiotechnol.* 2021;13:e1674.
 34. Chakraborty G, Park IH, Medishetty R, Vittal JJ. Two-dimensional metal–organic framework materials: synthesis, structures, properties and applications. *Chem Rev.* 2021;121:3751–891.
 35. Zhang X, Li G, Wu D, Li X, Hu N, Chen J, Chen G, Wu Y. Recent progress in the design fabrication of metal–organic frameworks-based nanozymes and their applications to sensing and cancer therapy. *Biosens Bioelectron.* 2019;137:178–98.
 36. Xiao Y, Chen C, Wu Y, Yin Y, Wu H, Li H, Fan Y, Wu J, Li S, Huang X, et al. Fabrication of two-dimensional metal–organic framework nanosheets through crystal dissolution-growth kinetics. *ACS Appl Mater Interfaces.* 2022;14:7192–9.
 37. Yuan A, Lu Y, Zhang X, Chen Q, Huang Y. Two-dimensional iron MOF nanosheet as a highly efficient nanozyme for glucose biosensing. *J Mater Chem B.* 2020;8:9295–303.
 38. Jiang ZW, Zhao TT, Li CM, Li YF, Huang CZ. 2D MOF-based photoelectrochemical aptasensor for SARS-CoV-2 spike glycoprotein detection. *ACS Appl Mater Interfaces.* 2021;13:49754–61.
 39. Sun L, Chen Y, Duan Y, Ma F. Electrogenerated chemiluminescence biosensor based on functionalized two-dimensional metal–organic frameworks for bacterial detection and antimicrobial susceptibility assays. *ACS Appl Mater Interfaces.* 2021;13:38923–30.
 40. Li J, Song S, Meng J, Tan L, Liu X, Zheng Y, Li Z, Yeung KWK, Cui Z, Liang Y, et al. 2D MOF periodontitis photodynamic ion therapy. *J Am Chem Soc.* 2021;143:15427–39.
 41. Zhuang S, Xiang H, Chen Y, Wang L, Chen Y, Zhang J. Engineering 2D Cu-composed metal–organic framework nanosheets for augmented nanocatalytic tumor therapy. *J Nanobiotechnol.* 2022;20:66.
 42. Castano AP, Mroz P, Hamblin MR. Photodynamic therapy and anti-tumour immunity. *Nat Rev Cancer.* 2006;6:535–45.
 43. Wang Y, Xu S, Shi L, Teh C, Qi G, Liu B. Cancer-cell-activated *in situ* synthesis of mitochondria-targeting AIE photosensitizer for precise photodynamic therapy. *Angew Chem Int Ed.* 2021;60:14945–53.
 44. Ni K, Lan G, Chan C, Quigley B, Lu K, Aung T, Guo N, La Riviere P, Weichselbaum RR, Lin W. Nanoscale metal–organic frameworks enhance radiotherapy to potentiate checkpoint blockade immunotherapy. *Nat Commun.* 2018;9:2351.
 45. Xie L, Zhang X, Chu C, Dong Y, Zhang T, Li X, Liu G, Cai W, Han S. Preparation, toxicity reduction and radiation therapy application of gold nanorods. *J Nanobiotechnol.* 2021;19:454.
 46. Sang W, Xie L, Wang G, Li J, Zhang Z, Li B, Guo S, Deng CX, Dai Y. Oxygen-enriched metal-phenolic X-ray nanoprocessor for cancer radio-radiodynamic therapy in combination with checkpoint blockade immunotherapy. *Adv Sci.* 2021;8:2003338.
 47. Wang W, Jin Y, Xu Z, Liu X, Bajwa SZ, Khan WS, Yu H. Stimuli-activatable nanomedicines for chemodynamic therapy of cancer. *Wiley Interdiscip Rev Nanomed Nanobiotechnol.* 2020;12:e1614.
 48. Xin J, Deng C, Aras O, Zhou M, Wu C, An F. Chemodynamic nanomaterials for cancer theranostics. *J Nanobiotechnol.* 2021;19:192.
 49. Zhao Y, Jiang L, Shangguan L, Mi L, Liu A, Liu S. Synthesis of porphyrin-based two-dimensional metal–organic framework nanodisk with small size and few layers. *J Mater Chem A.* 2018;6:2828–33.
 50. Lin Y, Wan H, Wu D, Chen G, Zhang N, Liu X, Li J, Cao Y, Qiu G, Ma R. Metal–organic framework hexagonal nanoplates: bottom-up synthesis, topotactic transformation, and efficient oxygen evolution reaction. *J Am Chem Soc.* 2020;142:7317–21.
 51. Cai X, Luo Y, Liu B, Cheng HM. Preparation of 2D material dispersions and their applications. *Chem Soc Rev.* 2018;47:6224–66.
 52. Yang X, Li S, Ikeda N, Sakuma Y. Oxide scale sublimation chemical vapor deposition for controllable growth of monolayer MoS₂ crystals. *Small Methods.* 2021;6:e2101107.

53. Ding Y, Chen YP, Zhang X, Chen L, Dong Z, Jiang HL, Xu H, Zhou HC. Controlled intercalation and chemical exfoliation of layered metal-organic frameworks using a chemically labile intercalating agent. *J Am Chem Soc.* 2017;139:9136–9.
54. He T, Ni B, Zhang S, Gong Y, Wang H, Gu L, Zhuang J, Hu W, Wang X. Ultrathin 2D zirconium metal-organic framework nanosheets: preparation and application in photocatalysis. *Small.* 2018;14:e1703929.
55. Cheng H, Liu Y, Hu Y, Ding Y, Lin S, Cao W, Wang Q, Wu J, Muhammad F, Zhao X, et al. Monitoring of heparin activity in live rats using metal-organic framework nanosheets as peroxidase mimics. *Anal Chem.* 2017;89:11552–9.
56. Huang Y, Zhao M, Han S, Lai Z, Yang J, Tan C, Ma Q, Lu Q, Chen J, Zhang X, et al. Growth of Au nanoparticles on 2D metallocporphyrinic metal-organic framework nanosheets used as biomimetic catalysts for cascade reactions. *Adv Mater.* 2017;29:1700102.
57. Qin L, Wang X, Liu Y, Wei H. 2D-metal-organic-framework-nanozyme sensor arrays for probing phosphates and their enzymatic hydrolysis. *Anal Chem.* 2018;90:9983–9.
58. Xia J, Xue Y, Lei B, Xu L, Sun M, Li N, Zhao H, Wang M, Luo M, Zhang C, et al. Multi-modal channel cancer chemotherapy by 2D functional gadolinium metal-organic framework. *Natl Sci Rev.* 2020;8:221.
59. Lan G, Ni K, Xu Z, Veroneau SS, Song Y, Lin W. Nanoscale metal-organic framework overcomes hypoxia for photodynamic therapy primed cancer immunotherapy. *J Am Chem Soc.* 2018;140:5670–3.
60. Ni K, Lan G, Chan C, Duan X, Guo N, Veroneau SS, Weichselbaum RR, Lin W. Ultrathin metal-organic-layer mediated radiotherapy-radiodynamic therapy. *Matter.* 2019;1:1331–53.
61. Ding Y, Chen Y, Xu N, Lian X, Li L, Hu Y, Peng S. Facile synthesis of FePS₃ nanosheets@MXene composite as a high-performance anode material for sodium storage. *Nanomicro Lett.* 2020;12:54.
62. Pustovarenko A, Goesten MG, Sachdeva S, Shan M, Amghouz Z, Belmabkhout Y, Dikhtierenko A, Rodenas T, Keskin D, Voets IK, et al. Nanosheets of nonlayered aluminum metal-organic frameworks through a surfactant-assisted method. *Adv Mater.* 2018;30:e1707234.
63. Zheng W, Tsang C-S, Lee LYS, Wong K-Y. Two-dimensional metal-organic framework and covalent-organic framework: synthesis and their energy-related applications. *Mater Today Chem.* 2019;12:34–60.
64. Fan Y, Zhang J, Shen Y, Zheng B, Zhang W, Huo F. Emerging porous nanosheets: from fundamental synthesis to promising applications. *Nano Res.* 2020;14:1–28.
65. Zeng Y, Wang M, Sun Z, Sha L, Yang J, Li G. Colorimetric immunosensor constructed using 2D metal-organic framework nanosheets as enzyme mimics for the detection of protein biomarkers. *J Mater Chem B.* 2022;10:450–5.
66. Wang Y, Mao Z, Chen Q, Koh K, Hu X, Chen H. Rapid and sensitive detection of PD-L1 exosomes using Cu-TCPP 2D MOF as a SPR sensitizer. *Biosens Bioelectron.* 2022;201:113954.
67. Lin Y, Li WH, Wen Y, Wang GE, Ye XL, Xu G. Layer-by-layer growth of preferred-oriented MOF thin film on nanowire array for high-performance chemiresistive sensing. *Angew Chem Int Ed.* 2021;60:25758–61.
68. Wang XY, Xiao SY, Jiang ZW, Zhen SJ, Huang CZ, Liu QQ, Li YF. An ultrathin 2D Yb(III) metal-organic frameworks with strong electrochemiluminescence as a “On-Off-On” platform for detection of picric acid and berberine chloride form. *Talanta.* 2021;234:122625.
69. Chen G, Bai W, Jin Y, Zheng J. Fluorescence and electrochemical assay for bimodal detection of lead ions based on metal-organic framework nanosheets. *Talanta.* 2021;232:122405.
70. Shi MY, Xu M, Gu ZY. Copper-based two-dimensional metal-organic framework nanosheets as horseradish peroxidase mimics for glucose fluorescence sensing. *Anal Chim Acta.* 2019;1079:164–70.
71. Quan W, Xudong W, Min X, Lou X, Fan X. One-dimensional and two-dimensional nanomaterials for the detection of multiple biomolecules. *Chin Chem Lett.* 2019;30:1557–64.
72. Alizadeh N, Salimi A, Hallaj R, Fathi F, Soleimani F. Ni-Hemin metal-organic framework with highly efficient peroxidase catalytic activity: toward colorimetric cancer cell detection and targeted therapeutics. *J Nanobiotechnol.* 2018;16:93.
73. Ling X, Gong D, Shi W, Xu Z, Han W, Lan G, Li Y, Qin W, Lin W. Nanoscale metal-organic layers detect mitochondrial dysregulation and chemoresistance via ratiometric sensing of glutathione and pH. *J Am Chem Soc.* 2021;143:1284–9.
74. Zhao L, Liu Y, Zhang Z, Wei J, Xie S, Li X. Fibrous testing papers for fluorescence trace sensing and photodynamic destruction of antibiotic-resistant bacteria. *J Mater Chem B.* 2020;8:2709–18.
75. Galvan DD, Yu Q. Surface-enhanced raman scattering for rapid detection and characterization of antibiotic-resistant bacteria. *Adv Healthc Mater.* 2018;7:e1701335.
76. Mankoff DA, Farwell MD, Clark AS, Pryma DA. Making molecular imaging a clinical tool for precision oncology: a review. *JAMA Oncol.* 2017;3:695–701.
77. Zhao W, Yu X, Peng S, Luo Y, Li J, Lu L. Construction of nanomaterials as contrast agents or probes for glioma imaging. *J Nanobiotechnol.* 2021;19:125.
78. Fu S, Cai Z, Ai H. Stimulus-responsive nanoparticle magnetic resonance imaging contrast agents: design considerations and applications. *Adv Healthc Mater.* 2021;10:e2001091.
79. Hsu JC, Nieves LM, Betzer O, Sadan T, Noel PB, Popovitz R, Cormode DP. Nanoparticle contrast agents for X-ray imaging applications. *Wiley Interdiscip Rev Nanomed Nanobiotechnol.* 2020;12:e1642.
80. Etrych T, Lucas H, Janouskova O, Chyttil P, Mueller T, Mader K. Fluorescence optical imaging in anticancer drug delivery. *J Control Release.* 2016;226:168–81.
81. Schouw HM, Huisman LA, Janssen YF, Slart R, Borra RJH, Willemse ATM, Brouwers AH, van Dijk JM, Dierckx RA, van Dam GM, et al. Targeted optical fluorescence imaging: a meta-narrative review and future perspectives. *Eur J Nucl Med Mol Imaging.* 2021;48:4272–92.
82. Meng X, Zhang K, Yang F, Dai W, Lu H, Dong H, Zhang X. Biodegradable metal-organic frameworks power DNAzyme for in vivo temporal-spatial control fluorescence imaging of aberrant MicroRNA and Hypoxic Tumor. *Anal Chem.* 2020;92:8333–9.
83. Ou YC, Wen X, Johnson CA, Shae D, Ayala OD, Webb JA, Lin EC, DeLapp RC, Boyd KL, Richmond A, et al. Multimodal multiplexed immunoimaging with nanostars to detect multiple immunomarkers and monitor response to immunotherapies. *ACS Nano.* 2020;14:651–63.
84. Meng HM, Shi X, Chen J, Gao Y, Qu L, Zhang K, Zhang XB, Li Z. DNA amplifier-functionalized metal-organic frameworks for multiplexed detection and imaging of intracellular mRNA. *ACS Sens.* 2020;5:103–9.
85. Zhu W, Yang Y, Jin Q, Chao Y, Tian L, Liu J, Dong Z, Liu Z. Two-dimensional metal-organic-framework as a unique theranostic nano-platform for nuclear imaging and chemo-photodynamic cancer therapy. *Nano Res.* 2019;12:1307–12.
86. Li R, Yuan S, Zhang W, Zheng H, Zhu W, Li B, Zhou M, Wing-Keung Law A, Zhou K. 3D printing of mixed matrix films based on metal-organic frameworks and thermoplastic polyamide 12 by selective laser sintering for water applications. *ACS Appl Mater Interfaces.* 2019;11:40564–74.
87. Zhong L, Chen J, Ma Z, Feng H, Chen S, Cai H, Xue Y, Pei X, Wang J, Wan Q. 3D printing of metal-organic framework incorporated porous scaffolds to promote osteogenic differentiation and bone regeneration. *Nanoscale.* 2020;12:24437–49.
88. Li X, Zhang C, Haggerty AE, Yan J, Lan M, Seu M, Yang M, Marlow MM, Maldonado-Lasuncion I, Cho B, et al. The effect of a nanofiber-hydrogel composite on neural tissue repair and regeneration in the contused spinal cord. *Biomaterials.* 2020;245:119978.
89. Ejelian F, Razmjou A, Nasr-Esfahani MH, Mohammad M, Karamali F, Ebrahimi Warkiani M, Asadnia M, Chen V. ZIF-8 modified polypropylene membrane: a biomimetic cell culture platform with a view to the improvement of guided bone regeneration. *Int J Nanomed.* 2020;15:10029–43.
90. Yao S, Wang Y, Chi J, Yu Y, Zhao Y, Luo Y, Wang Y. Porous MOF microneedle array patch with photothermal responsive nitric oxide delivery for wound healing. *Adv Sci.* 2021;9:e2103449.
91. Wang X, Sun X, Bu T, Wang Q, Zhang H, Jia P, Li L, Wang L. Construction of a photothermal hydrogel platform with two-dimensional PEG@Zirconium-ferrocene MOF nanozymes for rapid tissue repair of bacteria-infected wounds. *Acta Biomater.* 2021;135:342–55.
92. Chen G, Yu Y, Fu X, Wang G, Wang Z, Wu X, Ren J, Zhao Y. Microfluidic encapsulated manganese organic frameworks as enzyme mimetics for inflammatory bowel disease treatment. *J Colloid Interface Sci.* 2022;607:1382–90.
93. Yin Y, Yang J, Pan Y, Gao Y, Huang L, Luan X, Lin Z, Zhu W, Li Y, Song Y. Mesopore to macropore transformation of metal-organic framework

- for drug delivery in inflammatory bowel disease. *Adv Healthc Mater.* 2021;10:e2000973.
94. Wen T, Quan G, Niu B, Zhou Y, Zhao Y, Lu C, Pan X, Wu C. Versatile nanoscale metal–organic frameworks (nMOFs): an emerging 3D nanoplatform for drug delivery and therapeutic applications. *Small.* 2021;17:e2005064.
 95. Sui C, Tan R, Chen Y, Yin G, Wang Z, Xu W, Li X. MOFs-derived Fe-N codoped carbon nanoparticles as O₂-evolving reactor and ROS generator for CDT/PDT/PTT synergistic treatment of tumors. *Bioconjug Chem.* 2021;32:318–27.
 96. Zhao H, Huang J, Li Y, Lv X, Zhou H, Wang H, Xu Y, Wang C, Wang J, Liu Z. ROS-Scavenging hydrogel to promote healing of bacteria infected diabetic wounds. *Biomaterials.* 2020;258:120286.
 97. Yin M, Wu J, Deng M, Wang P, Ji G, Wang M, Zhou C, Blum NT, Zhang W, Shi H, et al. Multifunctional magnesium organic framework-based microneedle patch for accelerating diabetic wound healing. *ACS Nano.* 2021;15:17842–53.
 98. Xiao J, Zhu Y, Huddleston S, Li P, Xiao B, Farha OK, Ameer GA. Copper metal–organic framework nanoparticles stabilized with folic acid improve wound healing in diabetes. *ACS Nano.* 2018;12:1023–32.
 99. Liu X, Yan Z, Zhang Y, Liu Z, Sun Y, Ren J, Qu X. Two-dimensional metal–organic framework/enzyme hybrid nanocatalyst as a benign and self-activated cascade reagent for in vivo wound healing. *ACS Nano.* 2019;13:5222–30.
 100. Song Y, Yang J, Wang L, Xie Z. Metal–organic sheets for efficient drug delivery and bioimaging. *ChemMedChem.* 2020;15:416–9.
 101. Bieniek A, Wisniewski M, Czarnecka J, Wierzbicki J, Zietek M, Nowacki M, Grzanka D, Kłoskowski T, Roszek K. Porphyrin based 2D-MOF structures as dual-kinetic sorafenib nanocarriers for hepatoma treatment. *Int J Mol Sci.* 2021;22:11161.
 102. Lan G, Ni K, Veroneau SS, Feng X, Nash GT, Luo T, Xu Z, Lin W. Titanium-based nanoscale metal–organic framework for type I photodynamic therapy. *J Am Chem Soc.* 2019;141:4204–8.
 103. Zeng R, He T, Lu L, Li K, Luo Z, Cai K. Ultra-thin metal–organic framework nanosheets for chemo-photodynamic synergistic therapy. *J Mater Chem B.* 2021;9:4143–53.
 104. Jiang S, He Q, Li C, Dang K, Ye L, Zhang W, Tian Y. Employing the thiol-ene click reaction via metal–organic frameworks for integrated sonodynamic-starvation therapy as an oncology treatment. *Sci China Mater.* 2021. <https://doi.org/10.1007/s40843-021-1836-6>.
 105. Ni K, Luo T, Lan G, Culbert A, Song Y, Wu T, Jiang X, Lin W. A nanoscale metal–organic framework to mediate photodynamic therapy and deliver CpG oligodeoxynucleotides to enhance antigen presentation and cancer immunotherapy. *Angewandte Chemie Int Ed.* 2019;132:1124–8.
 106. Lu K, He C, Guo N, Chan C, Ni K, Weichselbaum RR, Lin W. Chlorin-based nanoscale metal–organic framework systemically rejects colorectal cancers via synergistic photodynamic therapy and checkpoint blockade immunotherapy. *J Am Chem Soc.* 2016;138:12502–10.
 107. Zheng Q, Liu X, Zheng Y, Yeung KW, Cui Z, Liang Y, Li Z, Zhu S, Wang X, Wu S. The recent progress on metal–organic frameworks for phototherapy. *Chem Soc Rev.* 2021;50:5086–125.
 108. Wu W, Pu Y, Lu X, Lin H, Shi J. Transitional metal-based noncatalytic medicine for tumor therapy. *Adv Healthc Mater.* 2021;10:e2001819.
 109. Luo T, Ni K, Culbert A, Lan G, Li Z, Jiang X, Kaufmann M, Lin W. Nanoscale metal–organic frameworks stabilize bacteriochlorins for type I and type II photodynamic therapy. *J Am Chem Soc.* 2020;142:7334–9.
 110. Lan G, Ni K, Veroneau SS, Luo T, You E, Lin W. Nanoscale metal–organic framework hierarchically combines high-Z components for multifarious radio-enhancement. *J Am Chem Soc.* 2019;141:6859–63.
 111. Lu K, He C, Guo N, Chan C, Ni K, Lan G, Tang H, Pelizzari C, Fu Y-X, Spiotto MT, et al. Low-Dose X-ray radiotherapy-radiodynamic therapy via nanoscale metal–organic frameworks enhances checkpoint blockade immunotherapy. *Nat Biomed Eng.* 2018;2:600–10.

Publisher's Note

Springer Nature remains neutral with regard to jurisdictional claims in published maps and institutional affiliations.

Ready to submit your research? Choose BMC and benefit from:

- fast, convenient online submission
- thorough peer review by experienced researchers in your field
- rapid publication on acceptance
- support for research data, including large and complex data types
- gold Open Access which fosters wider collaboration and increased citations
- maximum visibility for your research: over 100M website views per year

At BMC, research is always in progress.

Learn more biomedcentral.com/submissions

